



# Preparation of amino terminated polyamidoamine functionalized chitosan beads and its Cr(VI) uptake studies

Muniyappan Rajiv Gandhi, Sankaran Meenakshi\*

Department of Chemistry, Gandhigram Rural Institute (Deemed University), Gandhigram 624 302, Tamil Nadu, India

## ARTICLE INFO

### Article history:

Received 21 May 2012

Received in revised form 7 August 2012

Accepted 7 August 2012

Available online 17 August 2012

### Keywords:

Chitosan beads  
Polyamidoamine  
Protonation  
Chromium  
Sorption

## ABSTRACT

Chitosan beads, functionalized by amino terminated hyperbranched dendritic polyamidoamine (up to 3rd generation) were prepared by Michael addition of methyl acrylate to amino groups on the chitosan surface and amidation of terminal ester groups by ethylene diamine. All the three generation chitosan beads were used for chromium removal along with raw chitosan beads. However, the 3rd generation polyamidoamine chitosan beads (3ACB) have been protonated using HCl (3ACBP)/loaded with zirconium using  $\text{ZrOCl}_2 \cdot 8\text{H}_2\text{O}$  (3ACBZr) to enhance the sorption capacity towards Cr(VI). The zirconium loaded chitosan beads showed higher Cr(VI) sorption than the other modified chitosan beads. The zirconium loaded chitosan beads were characterized using SEM, EDAX, FT-IR, XRD, DSC and TGA. The system variables studied include agitation time, initial concentration of sorbate, pH, co-ions in the medium and temperature on the sorption of chromium. The chromium uptake onto 3ACBZr obeys the Freundlich isotherm. Thermodynamic studies revealed that the nature of chromium sorption is spontaneous and endothermic. The mechanism of chromium sorption onto the sorbent was established.

© 2012 Elsevier Ltd. All rights reserved.

## 1. Introduction

Chitosan, a deacetylated derivative of chitin, is a natural polymer, highly hydrophilic, nontoxic, abundant, biocompatible, and biodegradable polymer (Muzzarelli et al., 2012). Chemical modifications of a large numbers of hydroxyl and amino groups present in chitosan, can obviously improve the physical and chemical properties of chitosan and will open ways to various applications in different fields like biomedical, food ingredients and water treatment (Jayakumar et al., 2010; Tsubokawa & Takayama, 2000). In recent years, hyperbranched polymers, represented as dendrimer, have received great attention because of their multifunctional properties, morphological features and potential use in medical applications, host–guest chemistry, cosmetics, dendritic catalysts (Ravi Kumar, Muzzarelli, Muzzarelli, Sashiwa, & Domb, 2004; Sashiwa, Shigemasa, & Roy, 2002a, 2002b, 2002c). Modification of terminal groups with different functionalities, such as acetamido, hydroxyl, carboxyl, quaternary ammonium leads to the versatile applicability of chitosan as well as dendrimeric materials. Presently, a dendrimer like hyperbranched polyamidoamine was grafted onto the surface of chitosan and used for heavy metal removal (Ma et al., 2009; Qu et al., 2008). Our previous study shows that the

Cr(VI) sorption capacity of amino terminated hyperbranched dendritic polyamidoamine was very high when compare to protonated, carboxylated and amine grafted chitosan beads (Kousalya, Rajiv Gandhi, & Meenakshi, 2010). To increase the amino group in chitosan, dendritic chitosan was prepared. Further protonation of amino groups and rare earth metal ion loading increases the Cr(VI) removal than the aminated chitosan beads. The higher Cr(VI) sorption capacity of Zr(IV) loaded chitosan beads is due to its higher positive charge. Chitosan beads functionalized by  $\text{Zr}^{4+}$  loaded amino terminated hyperbranched dendritic polyamidoamine have not been reported for chromium removal. The probable mechanism of chromium sorption onto the sorbents was established.

## 2. Materials and methods

### 2.1. Materials

Chitosan (85% deacetylated) was supplied by Pelican Biotech and Chemicals Labs, Kerala (India). Ethylenediamine, methyl acrylate, acetic acid and  $\text{K}_2\text{Cr}_2\text{O}_7$  were purchased from Merck (India) and all other chemicals used were of analytical grade.

### 2.2. Instrumentation

The FT-IR samples were prepared by mixing 0.01 g of the crushed chitosan beads with 0.1 g of spectroscopy grade KBr and pressing the mixture under higher pressure. Under pressure, the

\* Corresponding author. Tel.: +91 451 2452371; fax: +91 451 2454466.

E-mail addresses: [rajivgandhi85@gmail.com](mailto:rajivgandhi85@gmail.com) (M. Rajiv Gandhi), [drs.meena@rediffmail.com](mailto:drs.meena@rediffmail.com) (S. Meenakshi).

KBr melts and seals the chitosan beads into a matrix. The FT-IR spectra were recorded using a JASCO-460 Plus FT-IR spectrometer in the wavenumber range of 400–4000  $\text{cm}^{-1}$  with a resolution of 4  $\text{cm}^{-1}$  in transmittance mode with 16 scans. The results of FT-IR spectroscopy was used to confirm the functional groups present, before and after Cr(VI) sorption onto the sorbents. The surface morphology of the sorbent was studied with scanning electron microscope (SEM), HITACHI-S-3400 model. Elemental spectra were obtained using an energy dispersive X-ray analyzer (EDAX) during SEM observations which allowed qualitative detection and localization of elements in the chitosan beads. X-ray diffraction (XRD) measurements were obtained using X'per PRO model-PANalytical to determine the crystalline phases present in sorbents. TGA and DSC were performed using a Setsys Evolution 16/18, under an oxygen flow with a heating rate of 5 K/min from 40 °C temperature to 400 °C.  $\text{pH}_{\text{zpc}}$  (pH of zero point charge) was determined by pH drift method in order to know the surface charge (Lopez-Ramon, Stoeckli, Moreno-Castilla, & Carrasco-Marin, 1999).

### 2.3. Preparation of modified chitosan beads

Chitosan beads were prepared, as suggested by Jeon and Holl (2003). Amino terminated hyperbranched dendritic polyamidoamine 1st generation (1ACB) chitosan beads was prepared by grafting reaction onto the chitosan beads by two processes. (1) Michael addition of methyl acrylate to amino groups on the surface and (2) amidation of terminal ester groups by ethylene diamine as reported (Ma et al., 2009; Qu et al., 2008; Tsubokawa and Takayama, 2000). 2nd generation chitosan beads (2ACB) and 3rd generation chitosan beads (3ACB) were prepared from 1ACB by repeating the above two processes. To enhance the Cr(VI) sorption capacity of 3ACB, it was protonated and loaded with Zr(IV). The 3ACB was protonated using con. HCl (3ACBP) and washed with water and then dried at room temperature. The loading of rare earth metal ions was carried out by treating 3ACB with 5% (W/V)  $\text{ZrOCl}_2 \cdot 8\text{H}_2\text{O}$  for 24 h and then washed with distilled water followed by drying at room temperature (3ACBZr). These dried beads were used for chromium sorption studies.

### 2.4. Cr(VI) adsorption experiments

Batch adsorption experiments were conducted by placing 100 mg of modified chitosan beads in 250 mL reagent bottles containing 100 mL of aqueous solution of Cr(VI) ions (200 mg/L) with different contact time. The effect of initial concentration of the Cr(VI) ion on the uptake by sorbents was carried out by placing 100 mg of modified chitosan beads in a series of flasks containing 100 mL of aqueous solution of Cr(VI) ions at definite concentrations and pH 4.0. The contents of the flasks were equilibrated on the shaker at 200 rpm for 200 min. Effect of different initial pH value were conducted by placing a 100 mg of modified chitosan beads in 250 mL reagent bottles containing 100 mL of aqueous solution of Cr(VI) ions (200 mg/L). The sample pH was adjusted to the desired value with hydrochloric acid or sodium hydroxide aqueous solution. The bottles were agitated at 200 rpm using a mechanical shaker for 200 min. After filtration, the Cr(VI) ions concentration in the filtrate and initial concentration were determined by UV–vis spectrometer and the adsorption capacities were calculated as follows:

$$\text{Sorption capacity (SC), } q = \frac{(C_0 - C_e)}{m} V \text{ mg/g} \quad (1)$$

where  $q$  is the adsorption capacities of modified chitosan beads (mg Cr(VI) ion/g adsorbent),  $V$  is the volume of Cr(VI) ion solution (L),  $C_0$  is the concentration of Cr(VI) ion before adsorption (mg/L),  $C_e$  is the concentration of Cr(VI) ion after adsorption (mg/L), and  $m$  is

the weight of sorbents (g). The effect of fivefold increase in concentration of competitor common ions was studied using an initial chromium concentration of 200 mg/L with the sorbent dosage of 100 mg/100 mL for 2 h. Adsorption isotherms were studied at different initial chromium concentrations viz., 50, 100, 150, 200 mg/L at different temperatures viz., 303, 313 and 323 K.

### 2.5. Analysis

The chromium(VI) ion concentration was measured using UV–vis spectrophotometer (Spectroquant Pharo 300 Merck) at 540 nm, according to the 1,5-diphenyl carbazide method (APHA, 2005). Duplicate measurements were made such that the residual concentration values were reproducible within  $\pm 2\%$ . The pH measurements were done with an expandable ion analyzer EA 940 with pH electrode (APHA, 2005).

## 3. Result and discussion

### 3.1. FT-IR analysis

Fig. 1a shows the FT-IR spectra obtained for 3ACB and 3ACBZr. 3ACB showed a broad band around 3419  $\text{cm}^{-1}$  corresponding to both primary amine and OH stretching groups of the chitosan moiety. Generally, primary amines will show two stretching bands around 3400–3300  $\text{cm}^{-1}$  and 3330–3250  $\text{cm}^{-1}$ . In contrast, this was not observed in the present case even though there was primary amine functionality in 3ACB. Instead a very broad band was observed. This may be due to the overlapping of the stretching bands of both primary amine and –OH groups present in 3ACB since –OH group also shows a broad and strong stretching band around 3500–3200  $\text{cm}^{-1}$ . In addition, in the region between 3500 and 3000  $\text{cm}^{-1}$ , there is the presence of the stretching vibrations of water molecules, present in the sample or in the atmosphere during the spectrum acquisition. Nevertheless, 3ACB clearly showed a sharp band at 1660  $\text{cm}^{-1}$  corresponding to the  $-\text{NH}_2$  bending mode of vibration. Further, 3ACB also showed two close bands with strong intensity at 1122  $\text{cm}^{-1}$  and 1058  $\text{cm}^{-1}$  corresponding to secondary and primary –OH stretching, respectively (Varma, Deshpande, & Kennedy, 2004). Amide groups in the chitosan molecule showed a stretching band of the amide  $-\text{C}=\text{O}$  around 1650  $\text{cm}^{-1}$  and the band at 1050–1100  $\text{cm}^{-1}$  are due to stretching vibrations of  $-\text{C}-\text{O}-\text{C}$  bonds of the glycosidic ring of chitosan beads. FT-IR spectrum of 3ACBZr showed the  $-\text{NH}_2$  bending at 1639  $\text{cm}^{-1}$  with a shift of 21  $\text{cm}^{-1}$  when compared to 3ACB (1660  $\text{cm}^{-1}$ ). This shift in  $-\text{NH}_2$  bending mode clearly confirms that Zr(IV) metal ion has been interacted with  $-\text{NH}_2$  group present in 3ACB. Further, the two bands at 1122  $\text{cm}^{-1}$  and 1058  $\text{cm}^{-1}$  corresponding to secondary and primary –OH stretching in 3ACB was also reduced to one band in 3ACBZr with a shift. This may be due to the interaction of primary –OH group of chitosan moiety with the Zr(IV) metal ion (Varma et al., 2004).

### 3.2. XRD

The XRD spectra of raw chitosan beads and 3ACBZr are shown in Fig. 1b. The chitosan beads showed two well defined peaks, i.e., a sharp peak at  $2\theta = 19.7^\circ$  and a broad peak around  $2\theta = 40^\circ$  (Rajiv Gandhi & Meenakshi, 2012). The raw chitosan beads also showed a weak shoulder around  $2\theta = 17^\circ$ . On the other hand, 3ACBZr (curve b) also showed 3 peaks. However, the position, intensity and nature of the peaks varied in contrast to chitosan beads. After loading with Zr(IV) metal ion, all the 3 peaks were decreased in intensity. The peak at  $2\theta = 19^\circ$  in chitosan bead was shifted to  $23^\circ$  after loading with Zr(IV) metal ion with comparable broadness in the peak, i.e., the incorporation of Zr(IV) metal ion

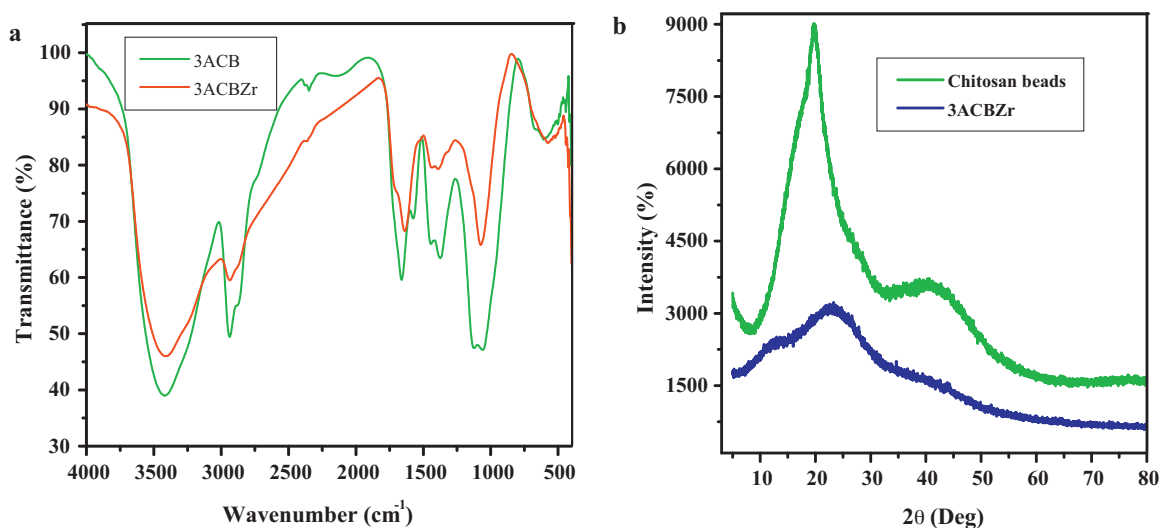


**Fig. 1.** (a) FT-IR spectra 3rd generation polyamidoamine chitosan beads and 3rd generation polyamidoamine chitosan beads loaded zirconium. (b) XRD spectra of chitosan beads and 3rd generation polyamidoamine chitosan beads loaded zirconium.

resulted in the significant decrease in the crystallinity of the bead. This observation may be explained by the strong absorption of X-rays by Zr(IV) metal ion in contrast to oxygen, carbon and other elements in raw chitosan. Thus, the change in crystalline nature of the chitosan bead after treating with Zr(IV) metal ions clearly confirms the incorporation of Zr(IV) metal ion into the chitosan beads.

### 3.3. Surface morphology

SEM was employed to analyze the surface morphology of 3ACBZr. Fig. 2a and b shows the SEM images of 3ACBZr micro photographed before sorption. This images shows that 3ACBZr is porous in nature and average size of the beads is 1.67 mm. Further, EDAX measurement was carried out to confirm the presence of Zr<sup>4+</sup>

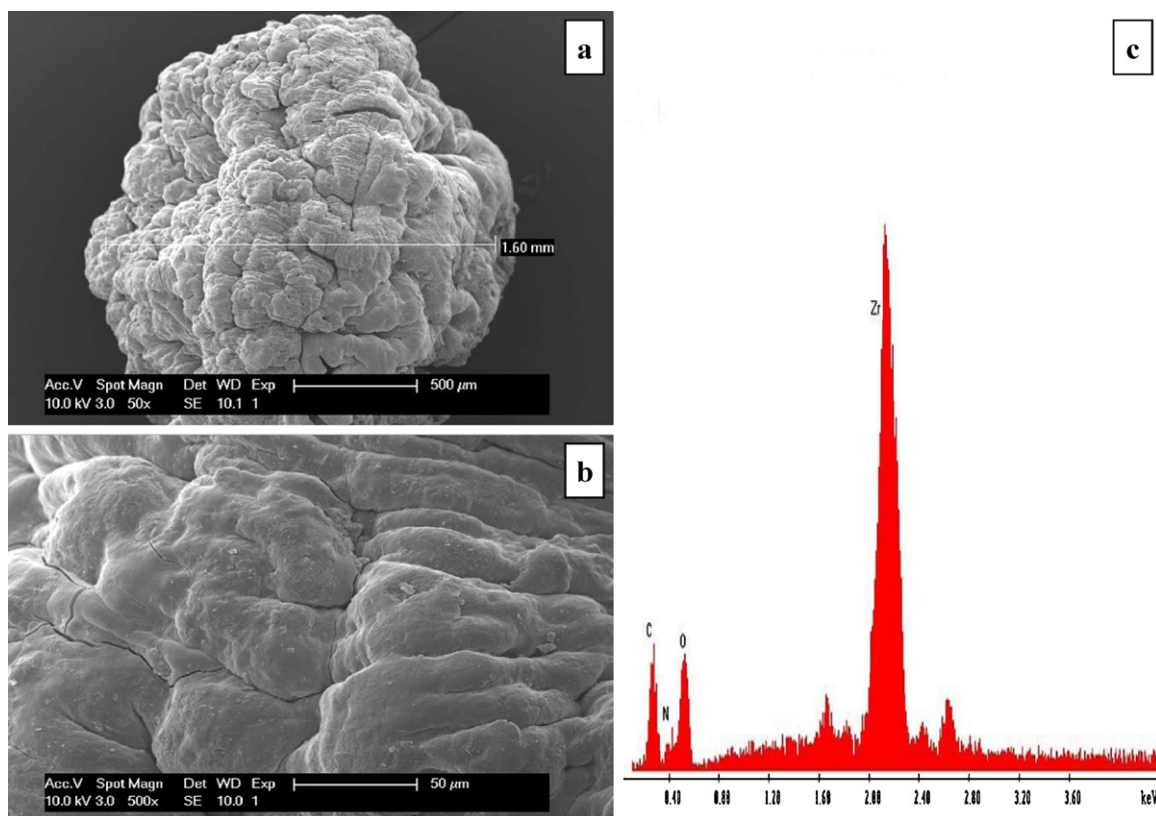


**Fig. 2.** SEM images (a and b) 3rd generation polyamidoamine chitosan beads loaded zirconium and (c) EDAX spectra of 3rd generation polyamidoamine chitosan beads loaded zirconium.

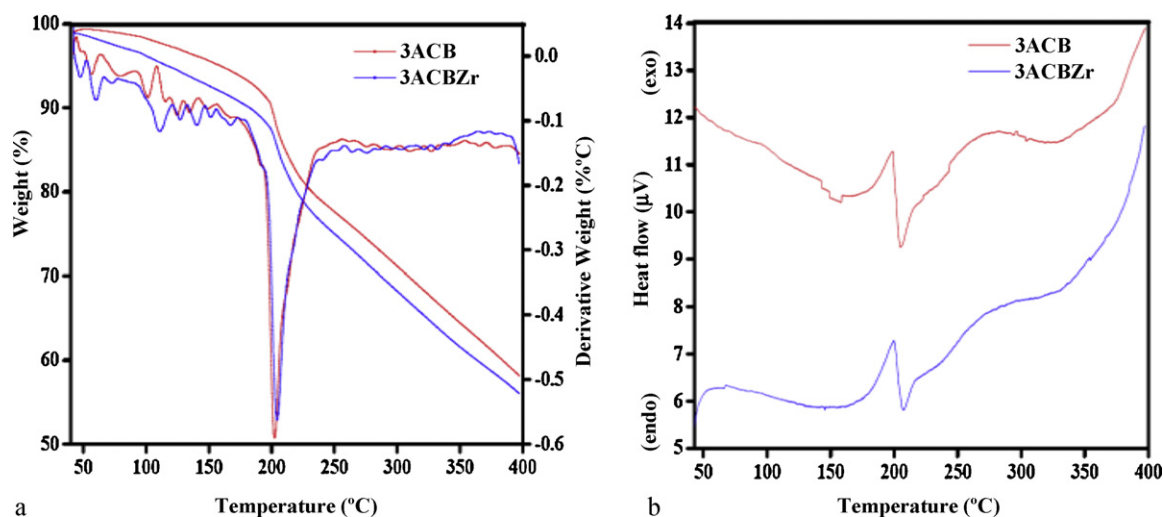


**Fig. 3.** (a) TGA/DTG thermogram of 3rd generation polyamidoamine chitosan beads and of 3rd generation polyamidoamine chitosan beads loaded zirconium; (b) DSC thermogram of 3rd generation polyamidoamine chitosan beads and 3rd generation polyamidoamine chitosan beads loaded zirconium.

ions in chitosan. Fig. 2c shows the peak for  $Zr^{4+}$  and the other peaks show the addition of other elements such as C, N and O present in chitosan. This clearly confirms the incorporation of  $Zr^{4+}$  ion into chitosan matrix.

#### 3.4. Thermogravimetric and differential scanning calorimetry studies

TGA/DTG thermogram of 3ACB and 3ACBZr is shown in Fig. 3a. The peak around 100°C is exothermic peak due to the evaporation of moisture present in the sorbent. The glass transition temperature of 3ACB and 3ACBZr is around 140–160°C. TGA/DTG thermogram clearly shows the considerable increase in the thermal stability of 3ACBZr compared to 3ACB. DSC thermogram of 3ACB and 3ACBZr is shown in Fig. 3b. The comparison of derivative thermograms of 3ACBZr and 3ACB implies that there was a shift towards higher temperature region (from 202°C to 204°C) after Zr loading with 3ACB. It clearly substantiates that 3ACBZr is thermally stable than 3ACB. The thermal degradation of sorbent was found to be single step. All the thermal trace was recorded in oxygen atmosphere.

#### 3.5. Metal adsorption studies

##### 3.5.1. pH and $pH_{zpc}$ studies

In all the pH ranges, Cr(VI) exist as  $HCrO_4^-$  and do not precipitate in wide pH ranges. The effect of pH was studied in entire ranges of pH values. As shown in Fig. 4, the higher uptake capacity was achieved at acidic pH values. The observed higher uptake in an acidic medium may be due to the electrostatic adsorption. In acidic medium 1ACB, 2ACB and 3ACB amine groups, partially protonated. The observed lower uptake in alkaline medium may be attributed to the competition of  $OH^-$  with  $HCrO_4^-$  ions on the modified chitosan beads. The higher Cr(VI) sorption capacity was observed in 3ACBZr when compared to the other modified forms of chitosan beads. 3ACBZr possess  $Zr^{4+}$  coordinated with amine groups and chromate ions adsorbed onto  $Zr^{4+}$ . The  $pH_{zpc}$  of chitosan beads is 7.6 where as for 1ACB and 3ACBZr it was shifted to 6.9 and 6.2, respectively which clearly indicate the occurrence of structural changes in the chitosan beads. The  $pH_{zpc}$  value of 3ACBZr was found to be 6.2. Lower SC in alkaline medium can be explained by the fact that above 6.2  $pH_{zpc}$  value the 3ACBZr surface acquires negative charge

in alkaline pH and hence there is repulsion between the negatively charged surface and  $HCrO_4^-$  and below 6.2  $pH_{zpc}$  value the sorbent surfaces attains positive charge and the negatively charged  $HCrO_4^-$  easily adsorbed.

##### 3.5.2. Effect of initial concentration of metal ions

Fig. 5 shows the uptake of Cr(VI) on modified chitosan beads at the solution pH of 4. The uptake of Cr(VI) ion on modified chitosan beads increases as the initial concentration increase up to 200 mg/L, thereafter there is no increase. The maximum uptake values of Cr(VI) at 200 mg/L initial concentration of Cr(VI) on chitosan beads, 1ACB, 2ACB, 3ACB, 3ACBP and 3ACBZr were 21.0, 60.0, 84.0, 105.0, 135.0 and 185.0 mg/g, respectively.

##### 3.5.3. Adsorption kinetics and effect of co-ions

Simple batch kinetic experiment of modified chitosan beads for the Cr(VI) ion adsorption was conducted (Fig. 6). It could be seen that the rate of adsorption of modified chitosan beads for Cr(VI) ion was high. Further, the experimental results suggest that the amount

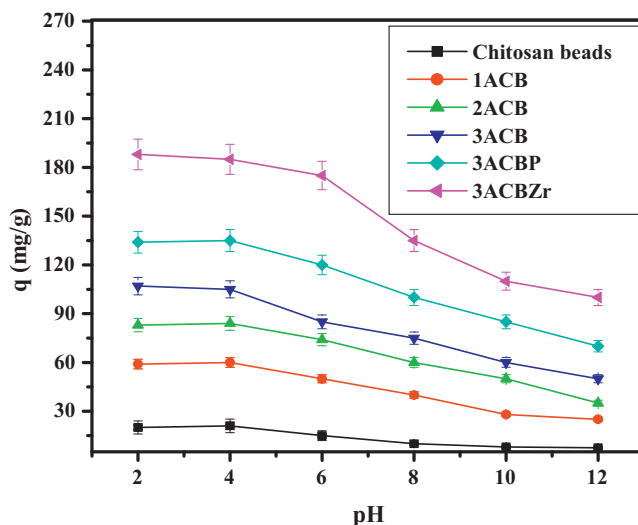


**Fig. 4.** Effect of pH on the uptake of Cr(VI) onto modified chitosan beads (Cr(VI) ion concentration: 200 mg/L, adsorbent dose: 1 g/L, contact t 2 h).



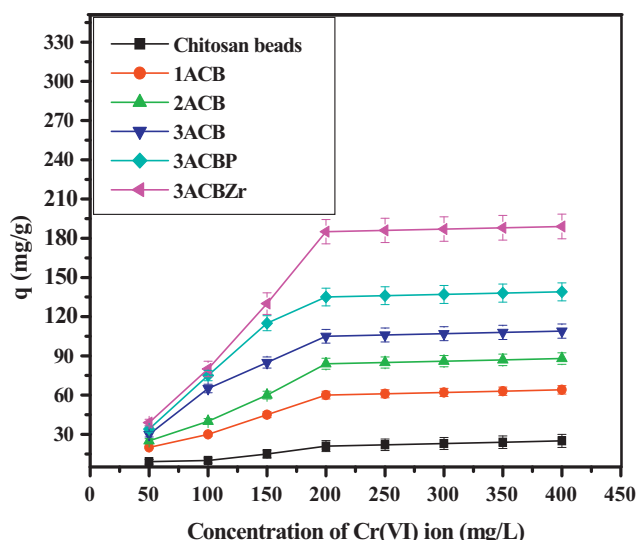


Fig. 5. Effect of initial concentration on the uptake of Cr(VI) by modified chitosan beads (pH: 4.0, adsorbent dose: 1 g/L).

of Cr(VI) adsorbed (mg/g) increased with the increasing contact time and reached equilibrium at 200 min. The heavy metal uptake potential may indicate that most of the active sites of modified chitosan beads are exposed for interaction with the Cr(VI) ion. The sorption capacity of 3ACBZr were studied in the presence of co-ion viz.,  $\text{Cl}^-$ ,  $\text{SO}_4^{2-}$ ,  $\text{HCO}_3^-$ ,  $\text{NO}_3^-$ ,  $\text{Ca}^{2+}$  and  $\text{Mg}^{2+}$  with concentration of co-ions as 1000 mg/L and with an initial chromium concentration of 200 mg/L. The cations viz.,  $\text{Ca}^{2+}$  and  $\text{Mg}^{2+}$  did not alter the SC of Cr(VI) on 3ACBZr, which remains as 185 mg/g as they are repelled by  $\text{Zr}^{4+}$  in aqueous solution. Anions like  $\text{SO}_4^{2-}$  and  $\text{HCO}_3^-$  have marginal interfering effect on the SC of Cr(VI) and were found to be 170 and 175 mg/g, respectively, while the interference of  $\text{NO}_3^-$  and  $\text{Cl}^-$  is not significant. This is due to the fact that these ions have ionic radius similar to that of  $\text{HCrO}_4^-$ . The same trend is found in the case of other sorbents reported by many authors (Kousalya et al., 2010; Rajiv Gandhi & Meenakshi, 2012). This confirms that the 3ACBZr is capable of removing Cr(VI) ions from aqueous solution selectively even in the presence of co-ions.

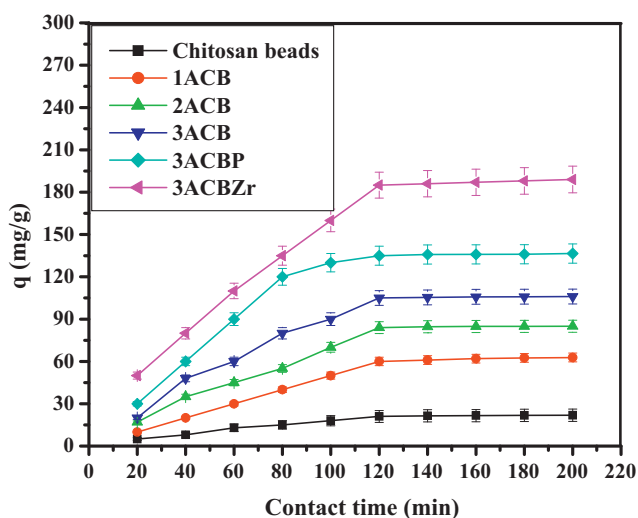


Fig. 6. Influence of contact time on the uptake of Cr(VI) by modified chitosan beads (Cr(VI) ion concentration: 200 mg/L, pH 4.0, adsorbent dose: 1 g/L).

### 3.6. Sorption isotherms

To quantify the sorption capacity of 3ACBZr for chromium sorption, three two-parameter equations namely Freundlich, Langmuir and D-R isotherms have been adopted.

#### 3.6.1. Freundlich isotherm

The linear form of Freundlich (1906) isotherm is represented by the equation,

$$\log q_e = \log k_F + \frac{1}{n} \log C_e \quad (2)$$

where  $q_e$  is the amount of chromium adsorbed per unit weight of the sorbent (mg/g),  $C_e$  is the equilibrium concentration of chromium in solution (mg/L),  $k_F$  is a measure of adsorption capacity and  $1/n$  is the adsorption intensity. A linear plot of  $\log q_e$  vs.  $\log C_e$  indicates the applicability of Freundlich isotherm. The values of  $n$ ,  $1/n$  and  $k_F$  of 3ACBZr are listed in Table 1. The values of  $1/n$  lying between 0 and 1 and the  $n$  value in the range of 1–10 confirm the favorable conditions for adsorption. The  $k_F$  values increased with the rise in temperature, which indicates that the chromium sorption by 3ACBZr is an endothermic process.

#### 3.6.2. Langmuir isotherm

Langmuir (1916) isotherm model can be represented by the equation

$$\frac{C_e}{q_e} = \frac{1}{Q^0 b} + \frac{C_e}{Q^0} \quad (3)$$

where  $Q^0$  is the amount of adsorbate at complete monolayer coverage (mg/g), which gives the maximum sorption capacity of the sorbent and  $b$  (L/mg) is the Langmuir isotherm constant that relates to the energy of adsorption. The linear plot of  $C_e/q_e$  vs.  $C_e$  indicates the applicability of Langmuir isotherm. The values of  $Q^0$  and  $b$  are listed in Table 1. The values of  $Q^0$  and  $b$  increase with the rise in temperature indicating the endothermic nature of chromium sorption. In order to find the feasibility of the isotherm, the essential characteristics of the Langmuir isotherm can be expressed in terms of a dimensionless constant separation factor or equilibrium parameter,  $R_L$  (Weber & Chakravorti, 1974).

$$R_L = \frac{1}{1 + bC_0} \quad (4)$$

where  $b$  is the Langmuir isotherm constant and  $C_0$  is the initial concentration of chromium (mg/L). The  $R_L$  values lying between 0 and 1 indicate favorable adsorption for all the temperatures studied (cf. Table 1).

#### 3.6.3. Dubinin–Radushkevich (D-R) isotherm

D-R isotherm was used to determine the type of adsorption for the removal of chromium from aqueous solution by adsorption (Karahan, Yurdakoc, Seki, & Yurdakoc, 2006). The equation can be expressed as

$$\ln q_e = \ln X_m - k_{DR} \varepsilon^2 \quad (5)$$

where  $X_m$  is the adsorption capacity (mg/g) and  $k$  is the constant related to adsorption energy ( $\text{mol}^2/\text{kJ}^2$ ). The values of  $k$  and  $X_m$  were computed from the slope and intercept of the plot  $\ln q_e$  vs.  $\varepsilon^2$ . Polanyi potential can be calculated by the equation,

$$\varepsilon = RT \ln \left( 1 + \frac{1}{C_e} \right) \quad (6)$$

where  $T$  is the temperature (K) and  $R$  is the gas constant ( $8.314 \text{ J mol}^{-1} \text{ K}^{-1}$ ). The value of  $k$  is used to calculate the mean free energy  $E$  (kJ/mol) of the sorption,

$$E = -(2k)^{-0.5} \quad (7)$$

**Table 1**  
Freundlich, Langmuir and Dubinin–Radushkevich isotherms parameters of 3rd generation polyamidoamine chitosan beads loaded zirconium(IV) for removal of Cr(VI).

Isotherms	Parameters	Temperature		
		303 K	313 K	323 K
Freundlich	$1/n$	0.727	0.791	0.818
	$n$	1.370	1.260	1.220
	$k_F$ (mg/g) (L/mg) $^{1/n}$	1.690	2.131	3.401
	$r$	0.999	0.999	0.998
	$\chi^2$	0.0238	0.0110	0.0178
Langmuir	$Q^0$ (mg/g)	224.2	249.3	265.2
	$b$ (L/g)	0.0038	0.0048	0.0074
	$R_L$	0.402	0.509	0.566
	$r$	0.976	0.997	0.987
	$\chi^2$	0.0882	0.0159	0.0187
Dubinin–Radushkevich	$k_{DR}$ (mol $^2$ /kJ $^2$ )	1.45E–08	1.43E–08	1.41E–08
	$X_m$ (mg/g)	181.2	198.3	200.3
	$E$ (kJ/mol)	5.872	5.912	5.954
	$r$	0.943	0.954	0.956
	$\chi^2$	0.161	0.183	0.201

The magnitude of  $E$  gives information about the type of adsorption/ion exchange mechanism.  $E$  value lying between 1–8 and 8–16 kJ/mol indicates the type of adsorption is physisorption and ion exchange, respectively. The linear plot of  $\ln q_e$  vs.  $\varepsilon^2$  with higher  $r$  values indicates the applicability of D–R isotherm. The values of  $k_{DR}$ ,  $X_m$ ,  $E$  and  $r$  are shown in Table 1.

The values of  $X_m$ , increase with the rise in temperature indicating the endothermic nature of chromium sorption. The obtained  $E$  values in this study lying between 1 and 8 kJ/mol indicate that the chromium removal was governed by electrostatic interaction which comes under the category of physisorption.

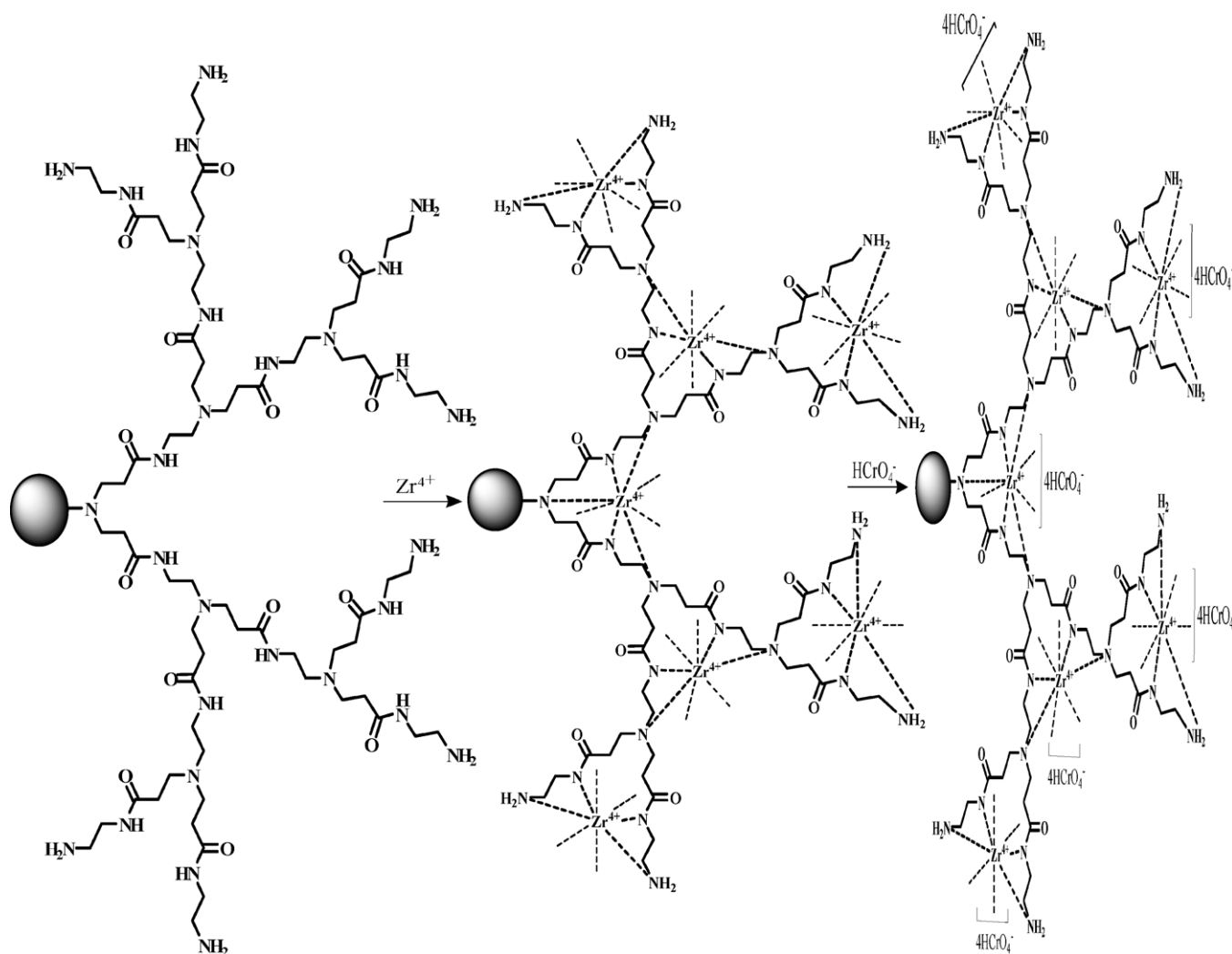


**Fig. 7.** Feasible mechanism of chromium sorption onto 3rd generation polyamidoamine chitosan beads loaded zirconium.

### 3.6.4. Chi-square analysis

To identify a suitable isotherm model for the sorption of chromium on 3ACBZr, this analysis has been carried out (Ho, 2004). The equivalent mathematical statement is

$$\chi^2 = \sum \frac{(q_e - q_{e,m})^2}{q_{e,m}} \quad (8)$$

where  $q_{e,m}$  is equilibrium capacity obtained by calculating from the model (mg/g) and  $q_e$  is experimental data of the equilibrium capacity (mg/g). If data from the model are similar to the experimental data,  $\chi^2$  will be a small number, while if they differ,  $\chi^2$  will be a bigger number. The results of chi-square analysis are presented in Table 1. The lower  $\chi^2$  values of Freundlich than the Langmuir and D–R isotherm isotherms suggest the applicability of best fitting model for the sorption of chromium on 3ACBZr.

### 3.7. Thermodynamic treatment of the sorption process

Thermodynamic parameters associated with the adsorption, viz., standard free energy change ( $\Delta G^\circ$ ), standard enthalpy change ( $\Delta H^\circ$ ) and standard entropy change ( $\Delta S^\circ$ ) were calculated as follows.

The free energy of sorption process, considering the sorption equilibrium coefficient  $K_0$ , is given by the equation

$$\Delta G^\circ = -RT \ln K_0 \quad (9)$$

where  $\Delta G^\circ$  is the standard free energy of sorption (kJ/mol),  $T$  is the temperature in Kelvin and  $R$  is the universal gas constant (8.314 J mol<sup>-1</sup> K<sup>-1</sup>). The sorption distribution coefficient  $K_0$ , was determined from the slope of the plot  $\ln(q_e/C_e)$  against  $C_e$  at different temperatures and extrapolating to zero  $C_e$  according to the method suggested by Khan and Singh (1987).

The sorption distribution coefficient may be expressed in terms of  $\Delta H^\circ$  and  $\Delta S^\circ$  as a function of temperature:

$$\ln K_0 = \frac{\Delta S^\circ}{R} - \frac{\Delta H^\circ}{RT} \quad (10)$$

where  $\Delta H^\circ$  is the standard enthalpy change (kJ/mol) and  $\Delta S^\circ$  is the standard entropy change (kJ/mol K). The values of  $\Delta H^\circ$  and  $\Delta S^\circ$  can be obtained from the slope and intercept of a plot of  $\ln K_0$  against  $1/T$ . The calculated values of thermodynamic parameters viz.,  $\Delta G^\circ$  was –13.20, –14.59, –15.57 kJ/mol at 303, 313 and 323 K, respectively,  $\Delta H^\circ$  was 22.89 kJ/mol and  $\Delta S^\circ$  was 0.11 kJ mol<sup>-1</sup> K<sup>-1</sup>. The negative values of  $\Delta G^\circ$  indicate the spontaneous nature of chromium sorption onto 3ACBZr. The value of  $\Delta H^\circ$  is positive indicating that the sorption process is endothermic. The positive value of  $\Delta S^\circ$  shows the increased randomness at the solid/solution interface during chromium sorption.

### 3.8. Mechanism of chromium removal

All modified chitosan beads removes chromium via adsorption (Kousalya et al., 2010). The percentage of chromium removal increases when the partial amino groups increases from 1ACB to 3ACB. The increased sorption capacity of 3ACBP is due to the complete protonation of amine groups. Further, Zr<sup>4+</sup> ion of 3ACBZr adsorbs higher chromate ion by electrostatic attraction. Feasible mechanism of chromium sorption onto 3ACBZr is given in Fig. 7.

## 4. Conclusions

3ACBZr possess higher SC than the other modified chitosan beads. This is because of the presence of more amine groups and Zr<sup>4+</sup> loading. The amount of Cr(VI) ions, adsorbed per unit mass

of adsorbents at 303 K from 200 mg/L of Cr(VI), by chitosan beads and 3ACBZr were 21 and 185 mg/g, respectively. All the sorbents need 200 min as the contact time for maximum SC. The SC of the sorbents was influenced by the pH of the medium. The maximum sorption capacity was at 2–4 pH. The sorption data follows Freundlich isotherm. The nature of sorption process is spontaneous and endothermic. These novel modified chitosan beads may have potential applications for the removal of Cr(VI) from water and wastewater.

## Acknowledgements

The corresponding author is grateful to the DRDO (No. ERIP/ER/0703670/M/01/1066), New Delhi, India for the financial support to carry out this research work. The first author likes to thank CSIR, New Delhi, India for awarding the SRF.

## References

- APHA. (2005). *Standard methods for the examination of water and waste water*. Washington, DC: American Public Health Association.
- Freundlich, H. M. F. (1906). Über die adsorption in lösungen. *Zeitschrift für Physikalische Chemie*, 57A, 385–470.
- Ho, Y. S. (2004). Selection of optimum sorption isotherm. *Carbon*, 42, 2115–2116.
- Jayakumar, R., Prabakaran, M., Nair, S. V., Tokura, S., Tamura, H., & Selvamurugan, N. (2010). Novel carboxymethyl derivatives of chitin and chitosan materials and their biomedical applications. *Progress in Polymer Science*, 55, 675–709.
- Jeon, C., & Holl, W. H. (2003). Chemical modification of chitosan and equilibrium study for mercury ion removal. *Water Research*, 37, 4770–4780.
- Karahan, S., Yurdakoc, M., Seki, Y., & Yurdakoc, K. (2006). Removal of boron from aqueous solution by clays and modified clays. *Journal of Colloid Interface Science*, 293, 36–42.
- Khan, A. A., & Singh, R. P. (1987). Adsorption thermodynamics of carbofuran on Sn(IV) arsenosilicate in H<sup>+</sup>, Na<sup>+</sup> and Ca<sup>2+</sup> forms. *Colloids and Surfaces*, 24, 33–42.
- Kousalya, G. N., Rajiv Gandhi, M., & Meenakshi, S. (2010). Sorption of chromium(VI) using modified forms of chitosan beads. *International Journal of Biological Macromolecules*, 47, 308–315.
- Langmuir, I. (1916). The constitution and fundamental properties of solids and liquids. *Journal of the American Chemical Society*, 38, 2221–2295.
- Lopez-Ramon, M. V., Stoeckli, F., Moreno-Castilla, C., & Carrasco-Marín, F. (1999). On the characterization of acidic and basic surface sites on carbons by various techniques. *Carbon*, 37, 1215–1221.
- Ma, F., Qu, R., Sun, C., Wang, C., Ji, C., Zhang, Y., et al. (2009). Adsorption behaviors of Hg(II) on chitosan functionalized by amino-terminated hyperbranched polyamidoamine polymers. *Journal of Hazardous Materials*, 172, 792–801.
- Muzzarelli, R. A. A., Boudrant, J., Meyer, D., Manno, N., DeMarchis, M., & Paoletti, M. G. (2012). Current views on fungal chitin/chitosan, human chitinases, food preservation, glucans, pectins and inulin: A tribute to Henri Braconnot, precursor of the carbohydrate polymers science on the chitin bicentennial. *Carbohydrate Polymers*, 87, 995–1012.
- Qu, R. J., Sun, C. M., Ji, C. N., Wang, C. H., Chen, H., Niu, Y. Z., et al. (2008). Preparation and metal-binding behaviour of chitosan functionalized by ester and amino-terminated hyperbranched polyamidoamine polymers. *Carbohydrate Research*, 343, 267–273.
- Rajiv Gandhi, M., & Meenakshi, S. (2012). Preparation and characterization of silica gel/chitosan composite for the removal of Cu(II) and Pb(II). *International Journal of Biological Macromolecules*, 50, 650–657.
- Ravi Kumar, M. N. V., Muzzarelli, R. A. A., Muzzarelli, C., Sashiwa, H., & Domb, A. J. (2004). Chitosan chemistry and pharmaceutical perspectives. *Chemical Reviews*, 104, 6017–6084.
- Sashiwa, H., Shigemasa, Y., & Roy, R. (2002a). Chemical modification of chitosan 8: Preparation of chitosan-dendrimer hybrids via short spacer. *Carbohydrate Polymers*, 47, 191–199.
- Sashiwa, H., Shigemasa, Y., & Roy, R. (2002b). Chemical modification of chitosan. Part 9: Reaction of *N*-carboxyethylchitosan methyl ester with diamines of acetal ending PAMAM dendrimers. *Carbohydrate Polymers*, 47, 201–208.
- Sashiwa, H., Shigemasa, Y., & Roy, R. (2002c). Chemical modification of chitosan 11: Chitosan-dendrimer hybrid as a tree like molecule. *Carbohydrate Polymers*, 49, 195–205.
- Tsubokawa, N., & Takayama, T. (2000). Surface modification of chitosan powder by grafting of dendrimer like hyperbranched polymer onto the surface. *Reactive and Functional Polymers*, 43, 341–350.
- Varma, A. J., Deshpande, S. V., & Kennedy, J. F. (2004). Metal complexation by chitosan and its derivatives: A review. *Carbohydrate Polymers*, 55, 77–93.
- Weber, T. W., & Chakravorti, R. K. (1974). Pore and solid diffusion models for fixed bed adsorbents. *Journal of American Institute of Chemical Engineers*, 20, 228–238.